International Conference on Renewable Energies and Power Quality (ICREPQ'19)
Tenerife (Spain), 10th to 12th April, 2019
Renewable Energy and Power Quality Journal (RE&PQJ)
ISSN 2172-038 X, No.17 July2019

Proposal of Novel Single-Phase Power Quality Indicators considering subsynchronous frequency perturbations in Voltage and Current under non-sinusoidal conditions.

[1]J. El Mariachet, [1]J. Matas, [1]H. Martin, [2]G. Tinoco, [1]S. Abdalinejad

[1] Department of Electrical Engineering, Universidad Politécnica de Cataluña (UPC), Barcelona, Spain.
[2] Department of Electrical Engineering, Universidad Michoacana. de San Nicolás de Hidalgo, Morelia, Mexico.

Abstract—**This work pretends to reconsider power quality (PQ), in AC single-phase low voltage systems, considering perturbation sources with frequency components below the fundamental frequency in voltage and current signals. These perturbations induced by sources like Geomagnetic Induced Currents (GMC), Arc Furnaces, switching VSC, etc. [1]-[2],[30]-[32], can occur in a frequency range comprised between DC and the fundamental frequency of the system. Standard PQ indexes do not characterize properly these subsynchronous frequency perturbations (SFFP), [2]-[3] and this work pretends to analyze the spectra from 0 to 50Hz for voltage and current, proposing new formulation for some PQ as a function of SSFP, with the intention of explaining the observed degradation of the power quality in single-phase low voltage electric systems.**

1. Introduction

Proposed and accepted Electric Power Theories (EPT), try to explain the energy flow in an Electric Power System (EPS), [5]-[9]. Since the adoption of these theories some PQ indexes have been defined in [3], [36], that are currently being considered for the measurement of energy consumption. However, following the evolution in distributed electric energy generation, storage and consumption, new PQ issues have appeared related to SSFP [6], [11], [12], particularly in single-phase microgrids. In this case, when supplying through voltage source inverters (VSI), Primary Level of Control algorithms are not properly solved because its control principles do not provide the correct state-variables information for the system performance, [13]-[15]. Even more, in the case of feeding non-linear loads [16]-[20], there is a range of frequency below the fundamental and close to DC which composition remains unexplained and, consequently, uncontrolled when the frequency domain electric power assumptions of [20]-[21] are adopted, not considering SSFP. Nevertheless, some VSI local control strategies where the measured voltage and current signals are conditioned by means of n-order Low Pass Filter (LPF), seem to work but only supplying to Linear Time Invariant (LTI) loads [17]-[19], [22]-[23].
Further attempts to establish an EPT have been developed since [20], that bring better explanations for understanding electric phenomena in single and three phase electrical grid. Among these hypotheses, the most widely accepted by the scientific community are the Instantaneous Power Theory of Akagi [10] with its p-q-r theory for single-phase and three-phase four wire systems, as well as the CPC of Czarnecki [24]. Firstly, Akagi et al. focused specifically in three-phase three-wire power systems, working under unbalanced conditions and supplying to LTI loads, but show to be inconsistent when considering NLTI loads and, consequently, it is not feasible for single-phase EPS. Secondly, CPC theory explains better electric system performance under non-sinusoidal conditions and establishes novel definitions for current components that point to the physical phenomena that causes them, but does not properly analyze the problem of the energy flow in the systems. Even more, in [25] interharmonic perturbances and subsyncronous frequency perturbations are not properly considered in the definition of a reactive and a scattered current. Later, some works developed strategies for control under non-sinusoidal conditions, but following a research method that is application-oriented as well as the state variables were not properly chosen [4], [26]-[27]. As a consequence of these EPT limitations, local control strategies in the referred cases SSFP are not sufficiently considered. Also some standards do not consider SSFP in its electric parameters and PQ indexes definitions [3], [36]. Finally, other authors tried to define power quality indexes in single-phase systems as a mean for defining power in three-phase four-wire systems, but do not correlate the power definitions and quality indicators to their causes or sources [4]. In Section 1 a state of the question is achieved in order to contextualize SSFP. Then, in Section 2 ideal and non-ideal voltage and current signals are formulated and different regions of the frequency spectra are parametrized. Section 3 instantaneous power spectra analysis is re-visited since [4]. In Section 4 formulation for some PQ indexes considering SSFP effects are proposed. Finally, Section 5 provides simulation results in order to evaluate existing and proposed PQ indexes

2. Characterization of SSFP

In terms of study of SSFP, Testa and others characterized it [26]. In the case of harmonics, this is a field widely studied in the literature. Nevertheless, the most important part of the experimental test and studies has been only focused in a small set of harmonic frequencies, because were related to the existing technology and associated phenomena of the EPS.
Thus, when calculating the instantaneous or averaged power for measuring or control purposes, the direct product of the time domain voltage and current signals will lead to a cross influence in between subharmonic, harmonic and interharmonic components. In terms of instantaneous power it

implies a large region for power configurations that could only be afforded by a selection of EPT in terms of approximation to the real events. In the case of the SSFP, these are acquiring a bigger importance in terms of energy amount injected to a single-phase EPS. For instance, the perturbations transmitted to the grid via the neutral point of the power transformers [28].

A. *Ideal Voltage and current Signals*

If we consider the definition of voltage and current below:

$$v(t) = V \cdot \sin(\omega \cdot t + \alpha) \quad (1)$$

$$i(t) = I \cdot \sin(\omega \cdot t + \beta) \quad (2)$$

where $v(t)$ and $i(t)$ are the expressions for voltage and current signals, respectively, in an AC circuit with an active-passive stochastic load (APS), see Fig. 1; ω is the frequency of the system, and α and β are phase angle for each signal referred to $t = t_{on}$. Considering an ideal voltage source, the current appears at (2) when the transference of energy to the APS load starts at $t_{on} = 0$. The APS load does not contain previously stored energy.

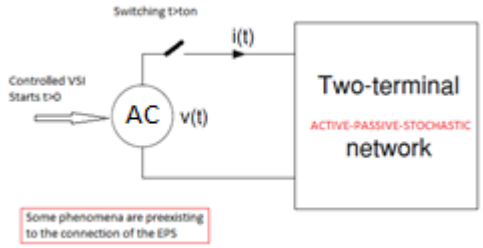

Fig. 1: Single-phase ideal EPS connecting a periodic voltage source to an active-passive stochastic load at $t_{on} = 0$

Considering only harmonic components of the fundamental frequency and a LTI load, (1) and (2) can be expressed in the form of Fourier Series:

$$v(t) = \sum_{h=0}^{+\infty} V_h \cdot \sin(h \cdot \omega_0 \cdot t + \alpha_h) \quad (3)$$

$$i(t) = \sum_{h=0}^{+\infty} I_h \cdot \sin(h \cdot \omega_0 \cdot t + \beta_h) \quad (4)$$

where $h \in Z$, ω_0 is defined as the fundamental frequency of the EPS, in rad/s, and I_h and V_h are the current and voltage amplitudes for each harmonic. The angles α_h and β_h are the phase shift for each voltage and current harmonic components. Note that the perturbations whose frequencies are comprised between h=0 and h=1 are not considered, which belong to the so-called subharmonic frequencies [3]. The same occurs with the frequencies in between one harmonic and the next in order, but this last appointment will be studied in further research. Note that, since [26], information between DC and fundamental frequencies is lost in the definitions of [3], [36].

B. *Non-ideal Voltage and current signals*

Equations (3) and (4) do not contain enough information about SSFP and are not suitable for the accurate calculation of electric power. In the present work a frequency threshold has been arbitrarily set somewhere between $\omega = 0$ and $= \omega_0$, for discrimination between periodic and non-periodic signals in EPS. Also, the spectra of frequencies is divided in three regions as indicated in Table 1 and shown in Fig. 2.

Table 1: Spectra of signals, Regions defined and some causes.

Frequency	REGION	Causes
$0 \leq \omega < w_{th}$	**#I DC Non-periodic time-dependent components (SSFP)**	GMC, Wind Farms shadow effect
$\omega_{th} < \omega < \omega_0$	**# II Sub-harmonic (SSFP)**	PWM switching, lightning flicker, Cyclic loads, Wind Farms Shadow Effect, etc.
$\omega \geq \omega_0$	**# III Harmonic**	Arc furnaces, Speed drives for motors, Lightning and PWM switching, etc.

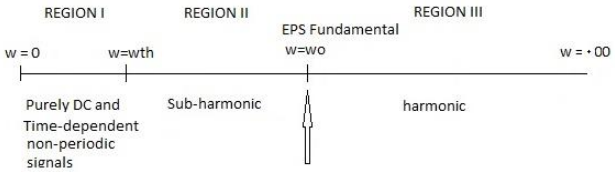

Fig. 2: Regions of the frequency spectra in an EPS accordingly with Table 1.

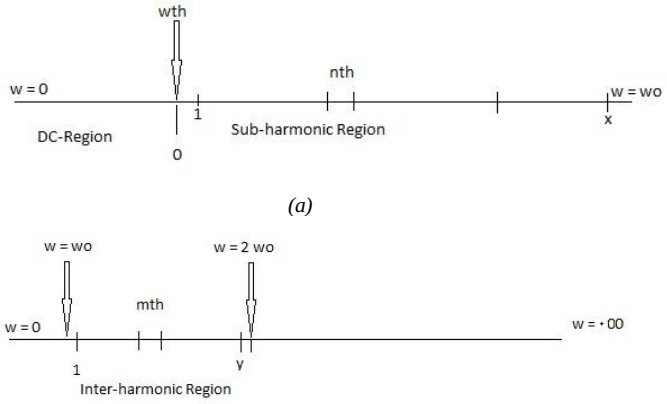

Fig. 3: a) Regions I and II of the spectra, from $\omega = 0$ to $= \omega_0$, where SSFP are present; b) Region III of the spectra, from $\omega = \omega_0$ to $\omega \to +\infty$, for definition of the Interharmonic frequencies.

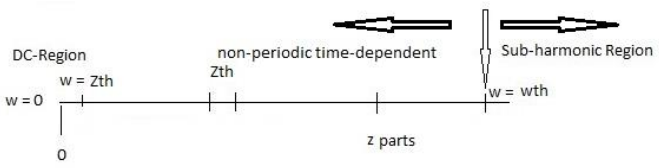

Fig. 4: Detail of Very Low Frequency, Non-periodic Time-Dependent and DC components region.

Region I includes at least frequencies compatibles with the shadow effect from wind turbines, 0.1–2.5 Hz [33], as well as with GMC that have frequencies that are in the range from 1mHz up to 1Hz [23], [34]-[35]. Following these frequency values for SSFP, a boundary between periodic and non-periodic SSFP needs to be set at $\omega_{th} = 10 \cdot \pi$ (rad/s). For these frequencies, the measurement concept based on IEC 61000-4-7 (10 cycles, 5Hz resolution, time window 200ms) cannot be properly applied [36], [37] as the time window should be at least of 50000 cycles for a 0.001Hz resolution, that makes it

unsuitable for local control of VSI in terms of dynamic performance. In this situation, the efficiency of FFT based on IEC 61000-4-7 standard suffers of the mentioned time window limitation, taking a too long interval for the extraction of the SSFP information for $\omega \leq \omega_{th}$. Then, for Region I there are only two parts: the purely-DC and the non-periodic time-dependent components. The last corresponds to the close-to-DC or quasi-DC phenomena indicated in the literature [28], [32]-[35]. In Fig. 2 it is depicted the region of frequencies below the fundamental. The dynamics of the called sub-harmonics in the literature are completely different to those in Region I. Because of this, Region II is analyzed by dividing its spectra in several parts, each one of a fixed frequency value compatible with the time windowing of a IEC 61000-4-7 based FFT, for instance. This determines the size of the frequencies, in which the maximum value and minimum frequency portion, depends on the resolution of the instrumentation. Therefore, in Region II, a fixed portion of frequency in rad/s, $\mathbf{n_{th}}$, is considered in order to define a set of $\boldsymbol{x}$ components named **SSFP-set** after the SSFP that occur in this region. Therefore, the minimum value of frequency is $\omega_{SSFPMIN} = \omega_{th}$ and the maximum value $\omega_{SSFPMAX}$ is determined by:

$$\omega_{SSFPMAX} < x \cdot n_{th} + \omega_{th} \quad (5)$$

$$x > \frac{\omega_0 - \omega_{th}}{n_{th}} - 1 \quad (6)$$

and only when fulfilling the following conditions:

$$\exists^{\cdot}\,(x, \omega_{th}) \leftrightarrow \left[\left(x = \frac{\omega_0 - \omega_{th}}{n_{th}}\right)\right];\ x \in Z\,; \\ ;(\omega_0 > (\omega_{th}, n_{th}) > 0) \epsilon \mathbb{R}^+ \quad (7)$$

$$\omega_{SSFPMAX} < \omega_0 \quad (8)$$

Then, the frequency of each element of the SSFP-set is determined as follows:

$$\omega_{th} < \omega = (\omega_{th} + x \cdot n_{th}) < \omega_{SSFPMAX} \quad (9)$$

$$\omega \neq \omega_0 \quad (10)$$

Note that some standards define its PQ indicators based on signals definitions as follows [3]:

$$i_o(t) = I_{DC} + I_0 \cdot \sin(\omega_o t + \beta_o) + \sum_{h=2}^{N} I_h \cdot \sin(h \cdot \omega_o t + \beta_h) \quad (11)$$

$$v_o(t) = V_{DC} + V_0 \cdot \sin(\omega_o t + \alpha_o) + \sum_{h=2}^{N} V_h \cdot \sin(h \cdot \omega_o t + \alpha_h) \quad (12)$$

Region III is the region for $\omega \geq \omega_0$ in which the frequencies between two consecutive multiples of the fundamental frequency have not been sufficiently modelled [18] for an APS, especially when fast transient phenomena take place. For its decomposition in Fourier series a set of non-integer multiples of fundamental frequency should be adopted for analytical purposes. Figure 3b shows the range of the region between two consecutive integer multiples of the fundamental frequency. In this range, a set of ***y*** elements is defined. The frequency of each element is not a multiple integer of the fundamental. The range of these frequencies is comprised between $m \cdot \omega_0 \leq \omega \leq (m+1) \cdot \omega_o$, where $m \in Z$. Therefore, a real value m_{th} has been stated, that :

$$m \cdot \omega_0 + y \cdot m_{th} < (m+1) \cdot \omega_0 \quad (13)$$

Note that $n_{th} \neq m_{th}$ and $x \neq y$, although:

$$y, n, m \in Z\,; (\omega_0 > m_{th} > 0) \epsilon R^+ \quad (14)$$

$$y < \frac{\omega_0}{m_{th}} \quad (15)$$

$$m_{th} \cdot (y+1) > \omega_0 \quad (16)$$

Equations (15) and (16) are the analytical expressions of the Inter-Harmonic Perturbations (IHP), contained in the IHP-set which size is *y*. This approach to the spectral analysis of voltage and current of the SSFP and IHP in EPS, leads to new expressions of the voltage and the current signals:

$$v(t) = V_{DC(t)} + \sum_{n=1}^{n=x} V_n \cdot \sin\big((\omega_{th} + n \cdot n_{th}) \cdot t + \alpha_n\big) + \sum_{m=1}^{+\infty} \sum_{k=0}^{k=y} V_k \cdot \sin((m \cdot \omega_0 + k \cdot m_{th}) \cdot t + \alpha_k) \quad (17)$$

$$i(t) = I_{DC(t)} + \sum_{n=1}^{n=x} I_n \cdot \sin\big((\omega_{th} + n \cdot n_{th}) \cdot t + \beta_n\big) + \sum_{m=1}^{+\infty} \sum_{k=0}^{k=y} I_k \cdot \sin((m \cdot \omega_0 + k \cdot m_{th}) \cdot t + \beta_k) \quad (18)$$

where $k \in Z$. Hence, three different regions A, B, C corresponding to the Regions I, II and III of Table 1 are presented for the sake of simplification:

$$v(t) = A_{V(t)} + B_{V(t)} + C_{V(t)} \quad (19)$$

$$i(t) = A_{i(t)} + B_{i(t)} + C_{i(t)} \quad (20)$$

As Region I is defined for very low frequencies, considering a sufficiently large time window for FFT analysis, the signal can be described as the sum of a constant value (DC) plus periodical sinusoidal components. But, when time window for this analysis is not large enough, we must consider it as a sum of DC and non-periodical time-dependent components. For this reason, under certain conditions, it can be applied the small-angle approximation to a sinusoidal signal and the expression will result as follows, for current:

$$A_{i(t)} = \sum_{l=0}^{l=z-1} I_l \cdot \beta_l + \frac{z_{th}}{z} \cdot t \cdot \sum_{l=0}^{l=z-1} l \cdot I_l \quad (21)$$

where $l \in Z$. A constant value $\sum_{l=0}^{l=z-1} I_l \cdot \beta_l$ and a non-periodical time-dependent signal, $\frac{z_{th}}{z} \cdot t \cdot \sum_{l=0}^{l=z-1} l \cdot I_l$,as predicted. The same study can be done for the voltage signal, obtaining these expressions:

$$A_{v(t)} = \sum_{l=0}^{l=z-1} V_l \cdot \alpha_l + \frac{z_{th}}{z} \cdot t \cdot \sum_{l=0}^{l=z-1} l \cdot V_l \quad (22)$$

Note that all the involved magnitudes are not predictable since its value is stochastic within their ranges, it is, theoretically unlimited for voltage and current and 0 to 2π for phase angle. Finally,

$$v(t) = \sum_{l=0}^{l=z-1} V_l \cdot \alpha_l + \frac{z_{th}}{z} \cdot t \cdot \sum_{l=0}^{l=z-1} l \cdot V_l + \sum_{n=1}^{n=x} V_n \cdot \sin\big((\omega_{th} + n \cdot n_{th}) \cdot t + \alpha_n\big) + \sum_{m=1}^{+\infty} \sum_{k=0}^{k=y} V_k \cdot \sin((m \cdot \omega_0 + k \cdot m_{th}) \cdot t + \alpha_k) \quad (23)$$

$$i(t) = \sum_{l=0}^{l=z-1} I_l \cdot \beta_l + \frac{z_{th}}{z} \cdot t \cdot \sum_{l=0}^{l=z-1} l \cdot I_l + \sum_{n=1}^{n=x} I_n \cdot \sin\big((\omega_{th} + n \cdot n_{th}) \cdot t + \beta_n\big) + \sum_{m=1}^{+\infty} \sum_{k=0}^{k=y} I_k \cdot \sin((m \cdot \omega_0 + k \cdot m_{th}) \cdot t + \beta_k) \quad (24)$$

Based on (17) and (18), it is important to note that the physical meaning of each expression must be proved. Each of the equations contains the information of the perturbations in amplitude and frequency of an EPS system with an APS load, indicated in Fig. 1.

3. Instantaneous Power Spectra

The energy flow through the system after $t > t_{on}$ depicted in Fig. 1 is

$$E_{(t)} = p_{(t)} \cdot t \quad (25)$$

Considering Table 2, the instantaneous power in the system can be calculated as the simple product of voltage and current, following the Budeanu's definition of instantaneous power in the frequency domain [20]:

$$p_{(t)} = v_{(t)} \cdot i_{(t)} \quad (26)$$

After that, and because of the distributive property:

$$p_{(t)} = AiAv + AiBv + AiCv + BiAv + BiBv + BiCv + CiAv + CiBv + CiCv \quad (27)$$

which gives the set of cells presented in Table 3 for a single-phase system. Although mathematically (27) is correct, each power cell should be related to its EPS phenomena as was intended in [19].

4. Novel THD Indexes Proposed for Region I

A novel set of PQ directly related to the SSFP both for Region I and II of Table 1 are proposed, under certain conditions. THD has been chosen because this index is directly related to the measured voltage and current and, following standards in [3] and [38], are the basis for other indexes as, for instance, Power Factor (PF). Then, for Region I, the voltage and current THD index could be presented as:

$$\mathrm{THD_{Av}} = \frac{\left|\sqrt{\frac{1}{cT}\int_0^{cT}\sum_{l=0}^{l=z-1}\left(V_l\cdot\alpha_l+\frac{z_{th}}{z}\cdot t\cdot l\cdot V_l\right)^2\cdot dt}\right|}{\left|\sqrt{\frac{1}{cT}\int_0^{cT}(V_0\cdot\sin(\omega_0\cdot t+\alpha_0))^2\cdot dt}\right|} \quad (28)$$

$$\mathrm{THD_{Ai}} = \frac{\left|\sqrt{\frac{1}{cT}\int_0^{cT}\sum_{l=0}^{l=z-1}\left(I_l\cdot\beta_l+\frac{z_{th}}{z}\cdot t\cdot l\cdot I_l\right)^2\cdot dt}\right|}{\left|\sqrt{\frac{1}{cT}\int_0^{cT}(I_0\cdot\sin(\omega_0\cdot t+\beta_0))^2\cdot dt}\right|} \quad (29)$$

where $c = \frac{\omega_0}{\omega_{th}} \gg 1$ and is related to the time window for measuring any non-periodic time dependent perturbation in current or voltage.

$$\mathrm{THD_{Bv}} = \frac{\left|\sqrt{\frac{1}{pT}\int_0^{pT}\sum_{n=1}^{n=x}(V_n\cdot\sin((\omega_{th}+n\cdot n_{th})\cdot t+\alpha_n))^2\cdot dt}\right|}{\left|\sqrt{\frac{1}{pT}\int_0^{pT}(V_0\cdot\sin(\omega_0\cdot t+\alpha_0))^2\cdot dt}\right|} \quad (30)$$

$$\mathrm{THD_{Bi}} = \frac{\left|\sqrt{\frac{1}{pT}\int_0^{pT}\sum_{n=1}^{n=x}(I_n\sin((\omega_{th}+n\cdot n_{th})\cdot t+\beta_n))^2\cdot dt}\right|}{\left|\sqrt{\frac{1}{pT}\int_0^{pT}(I_0\cdot\sin(\omega_0\cdot t+\beta_0))^2\cdot dt}\right|} \quad (31)$$

where p is defined as $p = \frac{\omega_0-\omega_{th}}{\omega_0} > 1$ and is related to the time window for measuring the sinusoidal components of Region II. Note that as $\omega_0 \gg \omega_{th}$, then c>p and it is to be considered at least c>10p.

5. Simulation Results

For the validation of the hypotheses, a simulation has been carried out consisting on a single-phase VSI connected to a Rectifier/R-C non-linear load, see Fig. 5. The architecture and the control scheme are explained in [16] and no changes in the power calculation had been introduced. Simulation parameters are listed in Table 4, where R is the resistance and C the capacitance after the rectifier, and $\xi_0; \xi_1; \xi_2$ are the damping factors of the local control loop conditioners for the calculation of active and reactive power. In [16] only a 3rd harmonic component was introduced in the voltage output of the VSI. The results of the calculated THD for current, voltage, active and reactive power, following the FFT tool in MATLAB/Simulink, are listed in Table 6. After that, a set of SSFP at 0.5Hz and at 0.25Hz components, both with 10% of the fundamental voltage amplitude, were added to the voltage source. Table 5 list these parameters. If the calculation of the $\boldsymbol{THD_{Av}}$ in ***(28)*** is analytically performed, it yields approximately a contribution of 1%. However, after carrying out the simulation considering voltage SSFP, the MATLAB/Simulink THD calculated through FFT for the voltage not only slightly decreases, it also shows contributions to THD in frequencies higher than 1Hz and below 50Hz, as can be seen in Table 7. Nevertheless, THD for output current varies, when SSFP in voltage are present, in spite of being conditioned through an 8th order BPF [16]. Even more, as Fig.6 shows, its influence on the reactive power is too strong, considering the variation in THD of reactive power shown in Table 6. This discrepancy reinforces the hypotheses formulated through Eq. (23), (24) and (27).

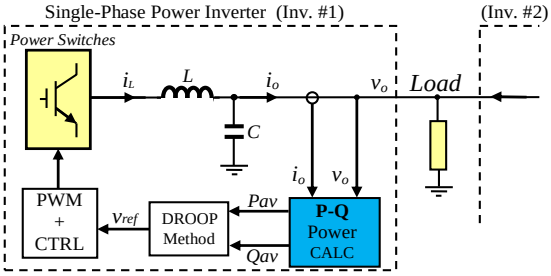

Fig. 5. Generic Droop-based control scheme of a single-phase inverter in [16].

Table 2: Regions of $v_{(t)}, i_{(t)}$ and potential sources

Region	Potential sources/effects
$A_{V\ (t)}$	Wind turbines shadow effect, GMC
$B_{V\ (t)}$	Cyclic Loads, Arc Furnaces, PWM controlled VSI
$C_{V\ (t)}$	Arc furnaces, Speed drives for motors, Lightning switching
$A_{i\ (t)}$	GMC, Wind turbines shadow effect
$B_{i\ (t)}$	Cyclic Loads Arc Furnaces PWM controlled VSI
$C_{i\ (t)}$	Arc furnaces Speed drives for motors Lightning switching

Table 3: Power cells and observable phenomena.

Power Cells	Product	Phenomena Associated
1	AiAv	SSFP
2	AiBv	SSFP
3	AiCv	HP
4	BiAv	SSFP
5	BiBv	SH
6	BiCv	IHP or SSFP
7	CiAv	Same than I
8	CiBv	Same than VI
9	CiCv	IHP

TABLE 4. SIMULATION PARAMETERS FOR FIG. 5.; [16]

$\boldsymbol{V_0}$	311V
$\boldsymbol{\omega_0}$	2π50(rad/s)
R ; C	1100Ω; 470μF
$\boldsymbol{\xi_0; \xi_1; \xi_2}$	0.7;1;1
$fc_{droop;}\ fc_{adv}$	1Hz; 10Hz

TABLE 5. SIMULATION SSFP IN VOLTAGE PARAMETERS

Amplitude(%)||V||	Frequency
10	$0.005 \cdot \omega_0$
10	$0.01 \cdot \omega_0$

TABLE 6. SIMULATION RESULTS.

THD current without/with SSFP	0.77% / 4.43%
THD voltage without/ with SSFP	5%/4.99%
Calculated $\boldsymbol{THD_{Av}}$ *(28)*	≈ 1%
THD Active Power without/with SSFP	0.53%/3.33%
THD Reactive Power without/with SSFP	12.39%/31.44%

Also active power ripple increases, which would mean a degradation of the Power Factor . Nonetheless, formulae for

calculation of PF in [3] do not consider SSFP, as it is based on the THD calculation of voltage and/or current described in (3) and (4). Moreover, SSFP due distortion is transmitted to the supposed averaged value of active power [16], [18], [29] through the product between (23) and (24) that leads to (27) and the power cells defined in Table 3. As it indicates, the model for calculation of active power with the only presence of odd and even harmonics at $\omega > \omega_0$ in [3], [6], [10], [20], [21], [24], [26], [32] is incompatible with the simulation results obtained. Again, reinforces the proposed model for non-sinusoidal voltage or current signals (23) and (24), which helps to explain where this PQ degradation is originated.

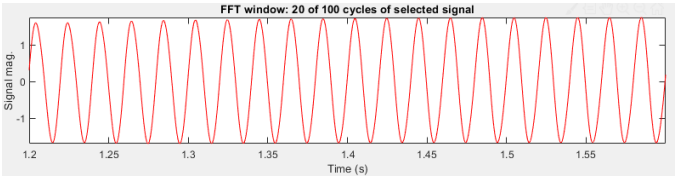

(a)

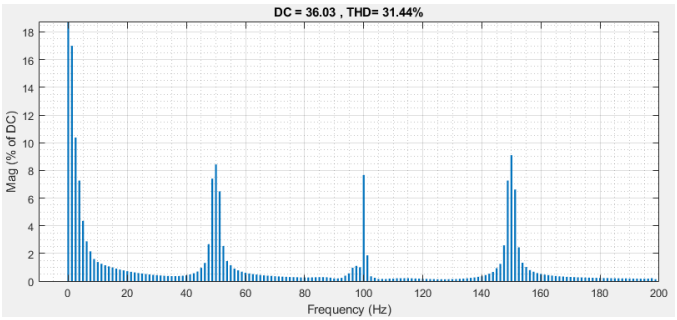

(b)

Fig. 6. Measured current at PCC: a) Output current filtered when SFFP present in voltage; b) Reactive power FFT with respect to DC component, in [16], after injecting SSFP in voltage

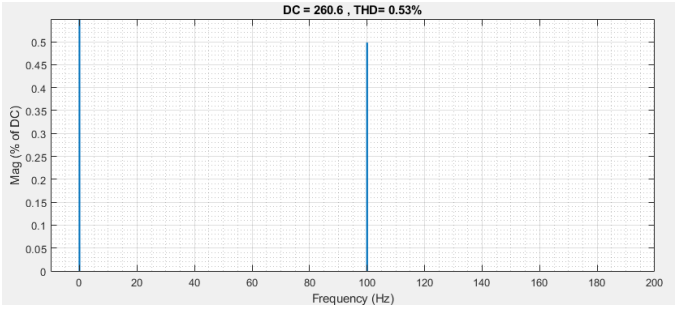

(a)

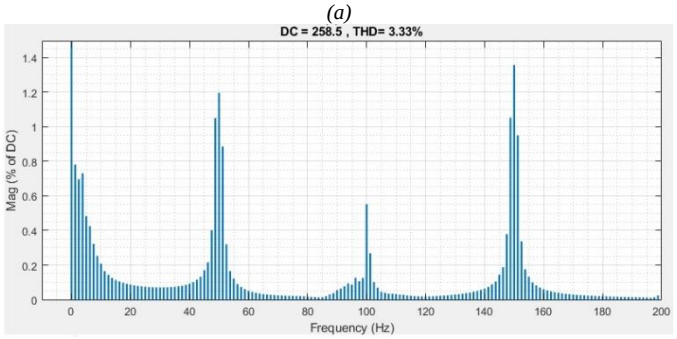

(b)

Fig. 7: Active power FFT spectra calculated with respect to the DC component: a) When SSFP in voltage are not introduced [16]; b) When SSFP are present in voltage, following Table 5.

TABLE 7. THD LIST FOR VOLTAGE BELOW 5HZ.

```
Sampling time     = 1e-05 s
Samples per cycle = 2000
DC component      = 6.271
Fundamental       = 310.3 peak (219.4 rms)
THD               = 4.99%

    0 Hz  (DC):          1.70%    270.0°
 1.25 Hz                 2.46%     67.9°
  2.5 Hz                 0.74%     41.4°
 3.75 Hz                 0.43%     29.2°
    5 Hz                 0.31%     22.4°
 6.25 Hz                 0.24%     18.1°
  7.5 Hz                 0.20%     15.2°
 8.75 Hz                 0.17%     13.1°
   10 Hz                 0.15%     11.6°
11.25 Hz                 0.13%     10.2°
 12.5 Hz                 0.12%      9.2°
13.75 Hz                 0.11%      8.4°
   15 Hz                 0.10%      7.7°
16.25 Hz                 0.09%      7.1°
 17.5 Hz                 0.08%      6.6°
18.75 Hz                 0.08%      6.2°
   20 Hz                 0.07%      5.8°
```

6. Conclusion

A model for studying SSFP in terms of resolution of measuring instrumentation had been tested both for non-sinusoidal voltage and current signals, (23) and (24). These models contain subsynchronous fundamental frequency information that is usually neglected by some standards and its PQ indexes traditionally employed [3], [36]. For frequencies higher than ω_{th} =5Hz, other indexes were proposed, THD_{Bv}, THD_{Bi}, THD_{Cv}, THD_{Ci},, but traditional FFT based on [36] may extract the same information and, although the initial hypotheses, it is considered that these indexes must be analysed in further works. However, (23), (24), (27) and (28) provide a better basis for spectral analysis of instantaneous Single-Phase power when SSFP are present [9]. For this purpose, the frequency spectra has been differentiated in three regions, see Figures 2, 3 and 4. In order to evaluate the new hypotheses, simulations considering a 3rd harmonic and SSFP introduced in voltage have been carried out. Then, the THD of the filtered non-linear load current shows a variation of 575.32%, see Table 6. Also, THD for the active power with respect to the DC component yields an increment of 628.30%; THD for the reactive power, yields an increment of 253.75%. However, THD in voltage is kept constant, see Table 6 and shows different weighting for the SSFP frequencies below 5Hz, see Table 7. This is not compatible with the calculated approximately 1% by means of the proposed THD_{Av} for Region I as well as there should not be contribution for frequencies higher than 0.5Hz, following the parameters of Table 4 and 5. These discrepancies demonstrates that appearance of SSFP at least in voltage degrades the active power calculation of [16], which is compatible with the lack of information of the signal model assumed in [3], [16], [18], [36], when supplying a nonlinear load. Studies considering different sources of SSFP, IHP and HP are planned to be carried out in order to characterize better all the proposed PQ indexes as well as the hypotheses behind (23), (24) and (27).

References

[1] S. Halász, "DC components and subharmonics of carrier-based PWM," *2012 15th International Power Electronics and Motion Control Conference (EPE/PEMC)*, Novi Sad, 2012, pp. DS3c.3-1-DS3c.3-7.

[2] Y. Denisov and S. Stepenko, "A subharmonic stability of power factor correctors with dual-loop control system," *2015 IEEE 35th International Conference on Electronics and Nanotechnology (ELNANO)*, Kiev, 2015, pp. 481-485.

[3] IEEE Standard Definitions for the Measurement of Electric Power Quantities Under Sinusoidal, Nonsinusoidal, Balanced, or Unbalanced Conditions - Redline," in IEEE Std 1459-2010 (Revision of IEEE Std 1459-2000) - Redline, vol., no., pp.1-52, March 19 2010.

[4] Hyosung Kim, F. Blaabjerg and B. Bak-Jensen, "Spectral analysis of instantaneous powers in single-phase and three-phase systems with use of p-q-r theory," in *IEEE Transactions on Power Electronics*, vol. 17, no. 5, pp. 711-720, Sept. 2002.

[6] L. S. Czarnecki, "On some misinterpretations of the instantaneous reactive power p–q theory," IEEE Trans. Power Electron., vol. 19, no. 3, pp. 828–836, May 2004.

[7] C.L. Fortescue, "Method of symmetrical coordinates applied to the solution of polyphase networks", *34th Annual Convention of the American Institute of Electrical Engineers*, June 1918.

[8] W. Shepherd, P. Zakikhani, "Suggested definition of reactive power for nonsinusoidal systems", *Proc. Inst. Electric. Eng.*, vol. 119, no. 9, pp. 1361-1362, 1972.

[9] Hyosung Kim, F. Blaabjerg and B. Bak-Jensen, "Spectral analysis of instantaneous powers in single-phase and three-phase systems with use of p-q-r theory," in *IEEE Transactions on Power Electronics*, vol. 17, no. 5, pp. 711-720, Sept. 2002.

[10] H. Akagi, Y. Kanazawa, A. Nabae, "Generalized theory of the instantaneous reactive power in three-phase circuit", *Proc. IPEC`83 Conf.*, pp. 1375-1386, 1983.

[11] Ch.P. Steinmetz, "Does phase displacement occur in the current of electric arcs?", *ETZ*, vol. 587, 1892.

[12] L. Cheng, W. Ki, F. Yang, P. K. T. Mok and X. Jing, "Predicting Subharmonic Oscillation of Voltage-Mode Switching Converters Using a Circuit-Oriented Geometrical Approach," in *IEEE Transactions on Circuits and Systems I: Regular Papers*, vol. 64, no. 3, pp. 717-730, March 2017.

[13] A. S. Chandran and P. Lenin, "A review on active & reactive power control strategy for a standalone hybrid renewable energy system based on droop control," *2018 International Conference on Power, Signals, Control and Computation (EPSCICON)*, Thrissur, 2018, pp. 1-10.

[14] T. Wu, G. Bao, Y. Chen and J. Shang, "A Review for Control Strategies in Microgrid,"*2018 37th Chinese Control Conference (CCC)*, Wuhan, 2018, pp. 30-35.

[15] Y. Han, H. Li, P. Shen, E. A. A. Coelho and J. M. Guerrero, "Review of Active and Reactive Power Sharing Strategies in Hierarchical Controlled Microgrids," in *IEEE Transactions on Power Electronics*, vol. 32, no. 3, pp. 2427-2451, March 2017.

[16] J. El Mariachet, J. Matas, Helena Martín, Abdullah Abusorrah, "Power Calculation Algorithm for Single-Phase Droop-Operated Inverters Considering Nonlinear Loads," in 2018 International Conference on Renewable Energies and Power Quality (ICREPQ), Salamanca, April 2018, pp.19-25.

[17] Guan, Y., Guerrero, J.M., Zhao, X., Vasquez, J.C., Guo, X. "A New Way of Controlling Parallel-Connected Inverters by Using Synchronous-Reference Frame Virtual Impedance Loop—Part I: Control Principle," Power Electronics, IEEE Transactions on, vol. 31, no. 6, pp: 4576 - 4593, June. 2016.

[18] S. Tolani and P. Sensarma, "An improved droop controller for parallel operation of single-phase inverters using R-C output impedance," *2012 IEEE Int. Conf. on Power Electronics, Drives and Energy Systems (PEDES)*, Bengaluru, 2012, pp. 1-6.

[19] Y. Yang and F. Blaabjerg, "A new power calculation method for single-phase grid-connected systems," *2013 IEEE International Symposium on Industrial Electronics*, Taipei, Taiwan, 2013, pp. 1-6.

[20] C.I. Budeanu, "Puissances reactives et fictives", Institut Romain de l'Energie Bucharest, 1927.

[21] S. Fryze, "Active reactive and apparent power in circuits with nonsinusoidal voltages and currents", *Przeglad Elektrotechniczny z.*, vol. 7, pp. 193-203, 1932.

[22] R. Guzman, L. G. de Vicuna, J. Morales, M. Castilla, J. Miret and J. Torres-Martinez, "Sliding-mode control for a three-phase shunt active power filter in natural frame," IECON 2015 - 41st Annual Conference of the IEEE Industrial Electronics Society, Yokohama, 2015, pp. 001211-001216.

[23] M. Soshinskaya, W. H. J. Graus, J. M. Guerrero, J. C. Vasquez, "Microgrids: experiences barriers and success factors", Renew. Sustain. Energy Rev., vol. 40, pp. 659-672, 2014.

[24] L.S. Czarnecki, "Orthogonal decomposition of the currents in a 3-phase nonlinear asymmetrical circuit with a nonsinusoidal voltage source", IEEE Trans. Instrum. Meas., vol. 1988, pp. 30-34, 1988.

[25] L. S. Czarnecki, "From steinmetz to currents' physical components (CPC): History of power theory development," 2016 International Conference on Applied and Theoretical Electricity (ICATE), Craiova, 2016, pp. 1-10.

[26] A. Testa and R. Langella, "Power system subharmonics," IEEE Power Engineering Society General Meeting, 2005, San Francisco, CA, 2005, pp. 2237-2242 Vol. 3.

[27] T. Keppler, N. R. Watson, J. Arrillaga and Shiun Chen, "Theoretical assessment of light flicker caused by sub- and interharmonic frequencies," in *IEEE Transactions on Power Delivery*, vol. 18, no. 1, pp. 329-333, Jan. 2003

[28] J. Fink, "Geomagnetic induced current in power transformers: A simplified model for the study of geomagnetic current spectra," *2017 IEEE International Conference on Computational Electromagnetics (ICCEM)*, Kumamoto, 2017, pp. 166-168.

[29] Rocabert, J.; Luna, A.; Blaabjerg, F.; Rodríguez, P., "Control of Power Converters in AC Microgrids," Power Electronics, IEEE Transactions on, vol.27, no.11, pp.4734,4749, Nov. 2012.

[30] D. H. Boteler and E. Bradley, "On the Interaction of Power Transformers and Geomagnetically Induced Currents," in *IEEE Transactions on Power Delivery*, vol. 31, no. 5, pp. 2188-2195, Oct. 2016.

[31] R. Langella, A. Testa, and A. E. Emanuel, "On the effects of subsynchronus interharmonic voltages on power transformers: Single phase units," IEEE Trans. Power Del., vol. 23, no. 4, pp. 2480–2487, Oct. 2008.

[32] Ewald F. Fuchs, Mohammad A.S. Masoum, "Power Quality in Power Systems and Electrical Machines", Associated Press, Aug. 29 2011, pp. 13-20, 191-195.

[33] Tan, Jin & Hu, Weihao & Wang, Xiaoru & Chen, Z. (2013). Effect of Tower Shadow and Wind Shear in a Wind Farm on AC Tie-Line Power Oscillations of Interconnected Power Systems. Energies. 6. 6352-6372. 10.3390/en6126352.

[34] S. Lu, Y. Liu, and J. De La Ree, "Harmonics generated from a DC biased transformer," IEEE Trans. Power Del., vol. 8, pp. 725-731, 1993.

[35] R. Pirjola, "Geomagnetically induced currents during magnetic storms," IEEE Trans. Power Del., vol. 28, pp. 1867-1873, 2000.

[36] IEC 61000 4-7, Electromagnetic compatibility (EMC) – Part 4-7: Testing and measurement techniques – General guide on harmonics and interharmonics measurements and instrumentation, for power supply systems and equipment connected thereto.

[37] Gunther, "Harmonic and Interharmonic Measurement According to IEEE 519 and IEC 61000-4-7," *2005/2006 IEEE/PES Transmission and Distribution Conference and Exhibition*, Dallas, TX, 2006, pp. 223-225.

[38] J. Arrillaga, Neville R. Watson, "Power systems Harmonics", Wiley, 2003, 2nd edition, pp. 47-56.

.